European Spine Journal (2024) 33:1713–1727
https://doi.org/10.1007/s00586-024-08163-3

ISSLS PRIZE

ISSLS PRIZE in Basic Science 2024: superiority of nucleus pulposus cell- versus mesenchymal stromal cell-derived extracellular vesicles in attenuating disc degeneration and alleviating pain

Luca Ambrosio[1,2,3] · Jordy Schol[3] · Clara Ruiz-Fernandez[3,4] · Shota Tamagawa[3,5] · Hazuki Soma[3] · Veronica Tilotta[2] · Giuseppina Di Giacomo[2] · Claudia Cicione[2] · Shunya Nakayama[6] · Kosuke Kamiya[6] · Rocco Papalia[1,2] · Masato Sato[3] · Gianluca Vadalà[1,2] · Masahiko Watanabe[3] · Vincenzo Denaro[1] · Daisuke Sakai[3]

Received: 13 October 2023 / Revised: 11 January 2024 / Accepted: 24 January 2024 / Published online: 28 February 2024
© The Author(s) 2024

Abstract

Purpose To investigate the therapeutic potential of extracellular vesicles (EVs) derived from human nucleus pulposus cells (NPCs), with a specific emphasis on Tie2-enhanced NPCs, compared to EVs derived from human bone marrow-derived mesenchymal stromal cells (BM-MSCs) in a coccygeal intervertebral disc degeneration (IDD) rat model.

Methods EVs were isolated from healthy human NPCs cultured under standard (NPC^{STD}-EVs) and Tie2-enhancing (NPC^{Tie2+}-EVs) conditions. EVs were characterized, and their potential was assessed in vitro on degenerative NPCs in terms of cell proliferation and senescence, with or without 10 ng/mL interleukin (IL)-1β. Thereafter, 16 Sprague–Dawley rats underwent annular puncture of three contiguous coccygeal discs to develop IDD. Phosphate-buffered saline, NPC^{STD}-EVs, NPC^{Tie2+}-EVs, or BM-MSC-derived EVs were injected into injured discs, and animals were followed for 12 weeks until sacrifice. Behavioral tests, radiographic disc height index (DHI) measurements, evaluation of pain biomarkers, and histological analyses were performed to assess the outcomes of injected EVs.

Results NPC-derived EVs exhibited the typical exosomal morphology and were efficiently internalized by degenerative NPCs, enhancing cell proliferation, and reducing senescence. In vivo, a single injection of NPC-derived EVs preserved DHI, attenuated degenerative changes, and notably reduced mechanical hypersensitivity. MSC-derived EVs showed marginal improvements over sham controls across all measured outcomes.

Conclusion Our results underscore the regenerative potential of young NPC-derived EVs, particularly NPC^{Tie2+}-EVs, surpassing MSC-derived counterparts. These findings raise questions about the validity of MSCs as both EV sources and cellular therapeutics against IDD. The study emphasizes the critical influence of cell type, source, and culture conditions in EV-based therapeutics.

Keywords Intervertebral disc · Disc degeneration · Extracellular vesicles · Exosomes · In vivo · Tie2

Luca Ambrosio and Jordy Schol have contributed equally to this work.

✉ Daisuke Sakai
daisakai@is.icc.u-tokai.ac.jp

1 Operative Research Unit of Orthopaedic and Trauma Surgery, Fondazione Policlinico Universitario Campus Bio-Medico, Rome, Italy

2 Research Unit of Orthopaedic and Trauma Surgery, Department of Medicine and Surgery, Università Campus Bio-Medico di Roma, Rome, Italy

3 Department of Orthopaedic Surgery, Tokai University School of Medicine, 143 Shimokasuya, Isehara 259-1193, Japan

4 NEIRID Lab (Neuroendocrine Interactions in Rheumatology and Inflammatory Diseases), IDIS (Instituto de Investigación Sanitaria de Santiago), Santiago University Clinical Hospital, Santiago de Compostela, Spain

5 Department of Medicine for Orthopaedics and Motor Organ, Juntendo University Graduate School of Medicine, Tokyo, Japan

6 Department of Hematological Malignancy, Institute of Medical Sciences, Tokai University, Isehara, Japan

Introduction

Low back pain (LBP) is the main cause of disability in the world [1] and is primarily triggered by intervertebral disc degeneration (IDD), a process characterized by catabolic events prompting extracellular matrix (ECM) degradation and cell loss, eventually altering disc morphology and biomechanics. To date, regenerative cell-based therapies are limited by poor post-transplantation viability, production scalability, and substantial donor variability [2]. Thus, cell-free therapeutics have been explored to overcome these hurdles. As anabolic effects exerted by transplanted cells are seemingly derived from their secretome, direct utilization of secreted factors may offer remarkable advantages over intradiscal cell delivery [3, 4]. In this context, extracellular vesicles (EVs) hold promise due to their role in intercellular communication and putative regenerative effects. With regard to IDD, mesenchymal stromal cell (MSC)-derived EVs have been demonstrated to reduce disc cell apoptosis, ECM degradation, tissue inflammation, and oxidative stress, both in vitro and in vivo [5].

Despite their notable chondrogenic potential, bone marrow-derived MSCs (BM-MSCs) exhibit significant differences from nucleus pulposus cell (NPC) progenitors [6], characterized by the expression of Tie2 receptors. Compared to $Tie2^{-}$-NPCs, these cells have demonstrated higher self-renewal, proliferation, viability, and multidifferentiation potential, as well as increased ECM production [7, 8]. Recent studies have also demonstrated that NPCs expressing Tie2 present a superior chondrogenic differentiation capacity compared to BM-MSCs [9]. However, the percentage of $Tie2^{+}$-NPCs is progressively exhausted with aging and advancing IDD, possibly explaining the limited ability of the IVD to perform self-repair [10].

Considering their regenerative capacity and recent advancements in culture methods to preserve Tie2 expression [11, 12], we sought to assess whether EVs secreted by this subpopulation might provide a promising cell-free therapy against IDD.

This study aimed to characterize and apply EVs derived from human NPCs cultured in standard and Tie2-enhancing conditions, to evaluate their biological effects in vitro, and to explore their regenerative potential in vivo.

Materials and methods

This study has been approved by the Institutional Review Board of Tokai University School of Medicine (Isehara, Kanagawa) under the approval number n. 221012. Informed consent for the collection and use of surgical waste products for research purposes was obtained from every patient. All animal experiments have been conducted according to the ARRIVE guidelines and in respect of the 3R principle. The detailed methodology is available as Supplementary Information.

Cell isolation and culture

Human IVD tissues were collected from surgical specimens at Tokai University Hospital (Isehara, Japan; Table 1). NPCs derived from young (mean age: 28.5 years) and healthy donors were cultured by standard

Table 1 Summary of characteristics of the donor IVD samples

Patient ID	Age (years)	Sex	Level(s)	Pfirrmann grade	Comorbidities	Application
1	*29*	*M*	*L5-S1*	*3/8*	–	Figures 3–9
2	*24*	*F*	*L4-L5, L5-S1*	*4/8*	*Depression*	Figures 3–9
3	*39*	*F*	*C4-C5, C5-C6*	*4/8*	–	Figures 3–5
4	*36*	*M*	*L4-L5*	*4/8*	–	Figures 3–5
5	*25*	*M*	*L4-L5*	*3/8*	–	Figures 3–5
6	*18*	*M*	*L5-S1*	*3/8*	–	Figures 3–5
7	48	F	C5-C6	5/8	Asthma	Figures 4–5
8	69	M	C3-C4	5/8	–	Figures 4–5
9	75	F	L2-L3, L3-L4	7/8	Diabetes, hypertension, rheumatoid arthritis	Figure 4
10	84	M	L3-L4	6/8	Hypertension	Figure 4
11	76	M	L4-L5	5/8	Diabetes, hypertension, dyslipidemia	Figure 4
12	59	M	C4-C5	7/8	Hypertension	Figure 4
13	71	M	L4-L5	6/8	Diabetes, hypertension, dyslipidemia	Figure 5

Age, sex, operated levels, Pfirrmann grade, and experiment allocation are listed

Italics indicate specimens exploited for extracellular vesicle (EV) isolation. IVD, intervertebral disc

non-Tie2-optimized (NPC^{STD}) or Tie2-enhancing culture strategies (NPC^{Tie2}; Fig. 1). Specimens were washed with phosphate-buffered saline (PBS), minced, and the NP tissue was carefully separated as previously described [7]. For NPC^{STD}, the tissue was digested in 0.25% trypsin–EDTA (Thermo Fisher, USA; 30 min, 37 °C), and then with 0.25 mg/mL collagenase P (Roche, Switzerland), Dulbecco's Modified Eagle Medium-High Glucose (DMEM-HG; Wako, Japan), and 10% fetal bovine serum (FBS, Sigma-Aldrich, USA; 4 h, 37 °C). The yielded suspension was filtered through an 80-µm cell strainer and seeded on standard 100-mm dishes (~ 1×10^5 cells/dish). Following the guidelines of the Orthopedic Research Society (ORS) [13], $NPCs^{STD}$ were cultured in DMEM-HG + 10% FBS + 1% penicillin/streptomycin (Gibco, USA) + 50 µg/mL L-ascorbic acid (Sigma-Aldrich) at 37 °C in 5% CO_2 and 5% O_2. The same protocol was adopted for NPCs from degenerative IVDs (dNPCs). After washing and mincing, the tissues undergoing the $NPCs^{Tie2+}$ culture approach were directly cultured in polystyrene six-well plates (IWAKI, Japan) with a commercially developed NPC-optimized, blended medium (MEMα:32%, DMEM:48%, FBS:20%; TUNZ Pharma Co., Ltd., Japan). Tissue fragments were cultured at 37 °C in 5% CO_2 and 5% O_2 for 14 days without media replenishment. Subsequently, cultured tissue fragments were digested as described above, and derived cells were seeded in monolayer at a density of 30,000 cells per 100-mm dish (545.5 cells/cm^2) using the same medium [11]. A commercial cell line of human BM-MSCs (Poietics™, Lonza, USA) was cultured in DMEM-HG + 10% FBS + 1% penicillin/streptomycin at 37 °C in 5% CO_2 and 21% O_2 (Fig. 1).

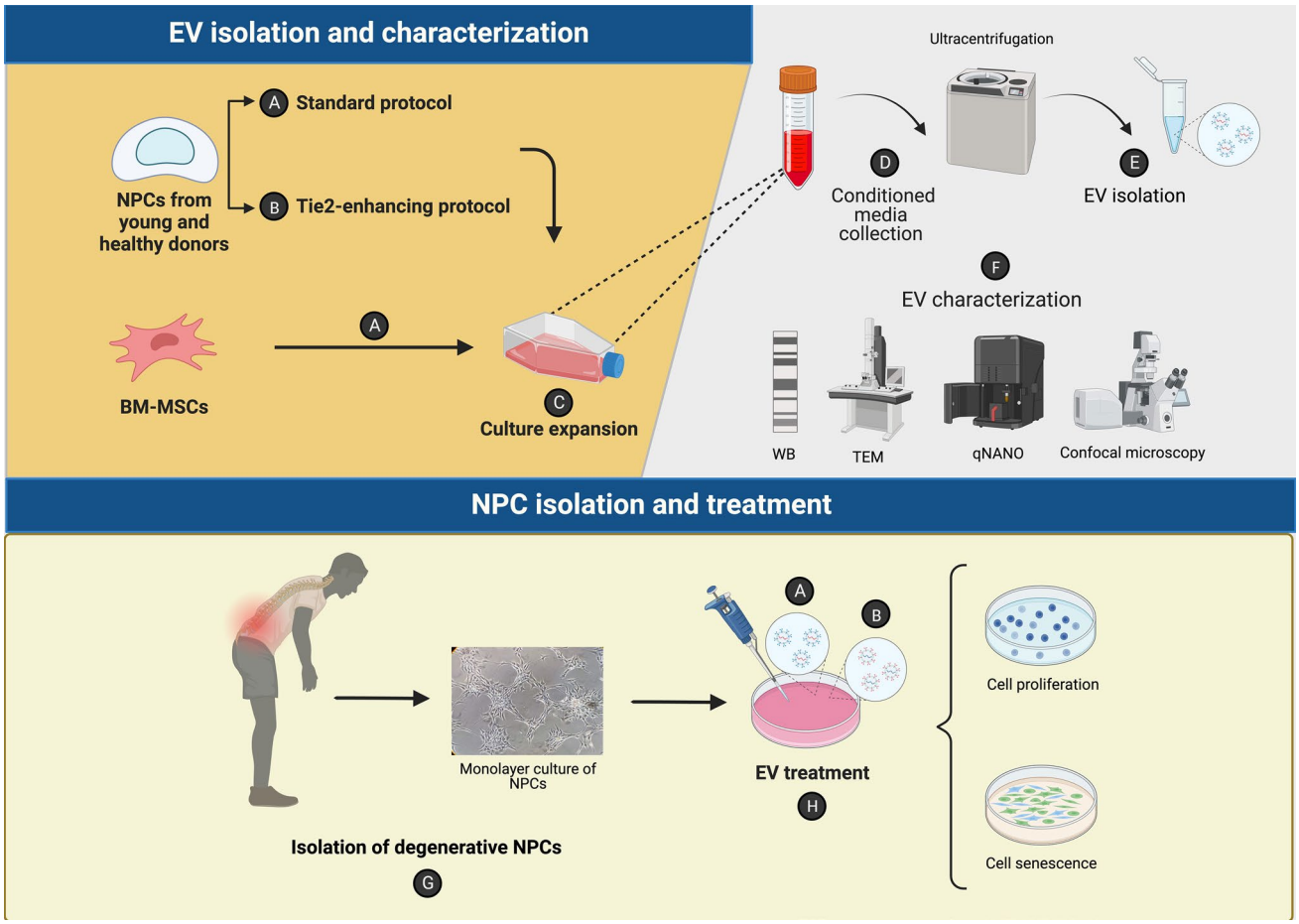

Fig. 1 Schematic design of the in vitro study. NPCs were isolated from young and healthy donors and cultured in monolayer according to either a standard (**a**) or a Tie2-enhancing (**b**) culture protocol. Human BM-MSCs were also cultured following standard methods. After culture expansion (**c**), conditioned media were collected (**d**) and processed for EV isolation (**e**) and subsequent characterization (**f**). Subsequently, degenerative NPCs were extracted from surgical specimens (**g**) and treated in vitro (**h**) with either EVs extracted from NPCs cultured in standard conditions (**a**) or in Tie2-enhancing conditions (**b**). Eventually, cell proliferation and senescence were assessed. Created with BioRender.com. Abbreviations: *BM-MSCs* bone marrow-derived stromal cells, *EV* extracellular vesicle, *NPCs* nucleus pulposus cells, *TEM* transmission electron microscopy, *WB* Western blot

EV isolation

FBS was ultracentrifuged (110,000 g for 17 h) and filtered through a 0.22-µm membrane to obtain bovine EV-free FBS [14]. $NPCs^{STD}$, $NPCs^{Tie2+}$, and BM-MSCs at 50–60% confluency were cultured with EV-free media for two days after which conditioned media were collected to isolate EVs as previously described [14]. Briefly, media were centrifuged at 1500 g (15 min), 12,000 g (30 min), and filtered with a 0.22-µm membrane to remove cell debris and larger vesicles. Eventually, the media were ultracentrifuged at 110,000 g (70 min) at 4 °C. The EV pellets were resuspended in PBS and ultracentrifuged again at 110,000 g (70 min) at 4 °C. The resulting EV products were used directly or stored at − 80 °C.

EV characterization

EV characterization was performed according to the International Society for Extracellular Vesicles guidelines [15], through transmission electron microscopy (TEM), single-particle analysis (qNano, Izon Science, New Zealand) [16] and assessment of CD63, CD9, TSG101, and lamin A/C expression by Western blot, comparing NPCs, BM-MSCs, and their EVs. EVs were quantified using the micro-bicinchoninic acid assay (Thermo Fisher).

EV uptake

NPCs were stained with Hoechst 33342 (Lonza), and isolated EVs were incubated with PKH26 (Sigma-Aldrich) for 5 min. Labeled EVs were applied onto NPCs for 180 min, and uptake was observed through confocal laser scanning microscopy (LSM700, Carl Zeiss, Germany).

EV effect in vitro

dNPCs were cultured using standard media ± 10 ng/mL IL-1β (PeproTech, USA) to further promote catabolism [17]. Both conditions were treated with NPC^{STD}-EVs or NPC^{Tie2+}-EVs at 25, 50, 75, and 100 µg/mL [18]. Dose–effect at days three and seven of culture was determined through the CCK-8 assay (Dojindo, USA). Cell proliferation was calculated as percent change compared to the DMEM-only group.

Cell senescence

dNPCs were seeded into six-well plates (2.5×10^5 cells/well) and treated for 72 h with or without IL-1β and/or 50 µg/mL EVs as explained above. Subsequently, cells were washed with PBS, fixed, and incubated overnight with β-galactosidase staining (Cell Signaling, USA). Cells were observed under a phase-contrast light microscope, capturing six random fields per well at 10 × magnification, to determine the proportion of positive cells to total cells in a blinded manner.

Western blot

EVs and intact cells were lysed in RIPA buffer (Thermo Fisher). Protein lysates were resolved by SDS-PAGE using NuPAGE 4–12% Bis–Tris Gel (Invitrogen), MES running buffer, and blotted onto PVDF membranes. Membranes were incubated with primary antibodies (1:1000) at 4 °C overnight and secondary antibodies (1:2000) at room temperature for 1 h. The primary antibodies used were: CD9 (sc13118, Santa Cruz Biotechnology, USA), CD63 (BD556019, BD Biosciences, USA), TSG101 (ab30871, Abcam, UK), lamin A/C (MAB3211, Sigma-Aldrich), and GAPDH (SAB2108668, Sigma-Aldrich). Immunoreactive bands were detected using an Amersham Healthcare ECL Prime Western Blotting Detection Reagent (Cytiva, Japan). Protein signals were quantified by scanning densitometry (ATTO, Japan).

Assessment of EVs on in vivo IDD

Sixteen Sprague–Dawley rats (10 to 12 weeks old, MIZUSETSU, Japan) were randomly assigned to sham ($n = 4$), NPC^{STD}-EV ($n = 4$), NPC^{Tie2+}-EV ($n = 4$), or BM-MSC-EV ($n = 4$) groups (Fig. 2). Males were chosen due to reduced behavioral variability [19]. Following acclimation and baseline data acquisition, IDD was induced by annular puncture from Co5/6 to Co7/8 as previously described [20]. Co4/5 and Co8/9 functioned as healthy controls. Discs were surgically exposed, and approximately 10 µL of NP tissue was aspirated with a 21G needle. Subsequently, 2 µL of either PBS-only (sham group), NPC^{STD}-EVs, NPC^{Tie2+}-EVs, or BM-MSC-EVs was injected through a 27G needle–Hamilton syringe combination. Approximately 1.5×10^6 EVs were injected per level [21].

Behavioral assessment

Behavioral tests were performed at baseline and biweekly post-transplantation as previously described [22, 23]. Animals were placed in a 60 × 60 cm open-field box and recorded for 10 min from a bird's eye view. The day before the test, animals were acclimatized in the enclosure for 10 min. Room lighting and time of day were kept consistent. EthoVision XT (Noldus Information Technology, The Netherlands) was used to analyze 18 parameters correlated with LBP as per previous studies [23].

The Von Frey test was performed using an esthesiometer (IITC, 2391). Three animals at a time were allowed

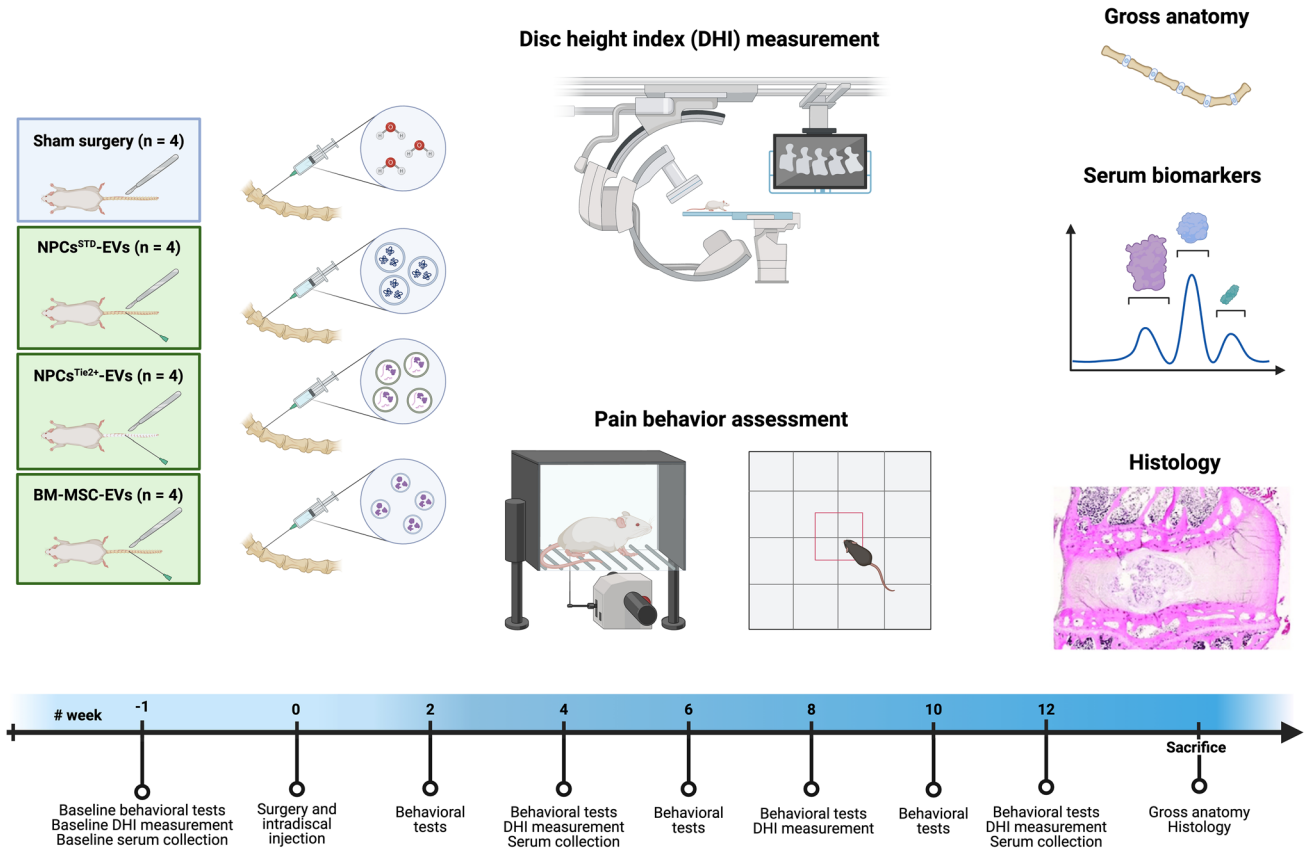

Fig. 2 Schematic design of the in vivo study. Sixteen Sprague–Dawley rats were randomly divided into four groups ($n=4$ per group), underwent annular puncture of three contiguous tail intervertebral discs, and subsequent injection of either PBS, NPC^{STD}-EVs, NPC^{Tie2+}-EVs, or BM-MSC-EVs. Animals underwent pain behavioral assessments (Von Frey test and open field test) every other week, radiographic evaluation of the DHI, and analysis of serum biomarkers at baseline, weeks 4, and 12. Following sacrifice, gross anatomy and histological analyses were carried out to evaluate disc structural changes. Abbreviations: *BM-MSC-EVs* extracellular vesicles isolated from bone marrow-derived mesenchymal stromal cells, *DHI* disc height index, *NPC^{STD}-EVs* extracellular vesicles isolated from nucleus pulposus cells cultured in standard conditions, *NPC^{Tie2+}-EVs* extracellular vesicles isolated from nucleus pulposus cells cultured in Tie2-enhancing conditions, *PBS* phosphate-buffered saline. Created with BioRender.com

to acclimate for 15 min in clear acrylic chambers placed on a metal grid. A maximum force of 28 g was applied ramping up over 10 s and kept for a maximum of 40 s. Withdraw threshold and time were assessed sequentially and alternatively by applying the probe on hind paws, tail base, and surgical site. This process was repeated at least thrice, and the averages were calculated. Investigators were blind to group allocation during the behavioral tests.

Serum biomarkers

Peripheral venous blood samples were obtained at baseline, 4, and 12 weeks post-operatively. Serum was isolated by centrifugation, frozen at − 80 °C, and used for IL-6 quantification using a rat-specific ELISA kit (RayBiotech, USA) as per the manufacturer's instructions.

Radiographic assessment

Radiographic assessment was conducted at baseline and 4, 8, and 12 weeks post-operatively. Images were obtained from the coccygeal region with the animals in the supine position using a fluoroscopic imaging intensifier (DHF-105CX, Hitachi, Japan) under 2.5% isoflurane inhalation. In a blinded manner, disc height index (DHI) was calculated and normalized to pre-transplantation DHI [24].

Macroscopic and histological evaluation

At 12 weeks, the animals were sacrificed, tails were dissected, and discs were explanted. Samples were fixed in 10% formalin and decalcified using Wako solution A (Wako). Functional spine units were sectioned and assessed through

Thompson grading system [25] by two blinded investigators. Subsequently, tissue sections were prepared for histology with hematoxylin/eosin, Safranin-O/Fast-Green, and Picrosirius-red/Aclian blue staining. Sections were blindly scored based on the ORS Spine rat histological grading scheme [26] by two investigators.

Statistical analysis

All quantitative data are expressed as means ± standard deviation. Data normal distribution was determined with the Wilk–Shapiro test. Statistical analysis was performed using one-way or two-way ANOVA. The Kruskal–Wallis test was performed to analyze non-normal data. Statistical significance was set as $p < 0.05$. Formal analysis was performed using Prism 10 (GraphPad, USA).

Results

EV isolation and characterization

TEM showed the typical EV oval cup morphology (Fig. 3a). NPC^{STD}-EVs, NPC^{Tie2+}-EVs, and BM-MSC-EVs exhibited an average diameter of 106.1 ± 16.3, 106.0 ± 18.2, and 87.0 ± 12.8 nm, respectively (Fig. 3b). The expression of EV markers CD63, CD9, and TSG101 was higher in EV samples compared to cell lysates, and lower for lamin A/C (Fig. 3c). PKH26-labeling showed EV uptake within NPCs (Fig. 3d). Collectively, these results demonstrated the isolation of small EVs (< 200 nm) with the characteristics of exosomes.

NPC^{STD}-EVs and NPC^{Tie2+}-EVs increased dNPC proliferation and reduced senescence

Dose–response evaluation of NPC^{STD}-EVs and NPC^{Tie2+}-EVs at day three showed that NPC^{Tie2+}-EVs significantly increased cell proliferation compared to NPC^{STD}-EVs at all concentrations ($p < 0.05$). Interestingly, the addition of IL-1β to NPC^{STD}-EVs ($p < 0.05$) and NPC^{Tie2+}-EVs ($p < 0.01$) further enhanced cell proliferation compared to NPC^{STD}-EVs alone (Fig. 4a). Similar results were observed at day seven (Fig. 4b). dNPCs treated with IL-1β showed an elongated, fibroblastic-like conformation, while NPC^{STD}-EV- and NPC^{Tie2+}-EV-treated cells exhibited a preserved morphology, even in the presence of IL-1β (Fig. 4c). Considering the lack of significant differences among tested EV concentrations, the intermediate value (50 µg/mL) was utilized in subsequent experiments. β-galactosidase staining (Fig. 5) demonstrated that NPC^{STD}-EVs and NPC^{Tie2+}-EVs significantly decreased senescent cell ratio compared to dNPCs cultured with IL-1β ($p < 0.05$). Furthermore, NPC^{Tie2+}-EVs prevented IL-1β-induced senescence ($p < 0.05$).

NPC-EVs decreased mechanical hypersensitivity and modulated pain-like behaviors in vivo

IDD induction and transplantation procedures were successfully performed without complications. Animals displayed stable weight without discernible differences among cohorts (Supplementary Fig. 1). The Von Frey test demonstrated that NPC^{STD}-EVs and NPC^{Tie2+}-EVs significantly lowered the nocifensive response threshold compared to the sham and BM-MSC-EV groups at the surgical site (Fig. 6a) and tail base (Fig. 6B; $p < 0.05$). Interestingly, NPC^{Tie2+}-EV-treated rats consistently exhibited the highest pain threshold and time until withdrawal (Supplementary Fig. 2a). No statistically significant differences were found following sham or BM-MSC-EV injections. No mechanical hypersensitivity was demonstrated for hind paws in any tested groups (Supplementary Fig. 2b).

The open field test, aimed to assess changes in spontaneous pain-like behavior, showed no evident between-group differences. Rats in the NPC^{STD}-EV and NPC^{Tie2+}-EV groups showed higher mean velocity, total distance, movement duration, behavioral probability of walking and rearing unsupported, walking frequency, and rearing unsupported duration and frequency, albeit failing to reach statistical significance (Fig. 7a–r). Although not showing significant differences, IL-6 serum levels displayed a more substantial decrease in NPC^{Tie2+}-EV-injected animals compared to the other groups (Fig. 7S).

NPC^{STD}-EVs and NPC^{Tie2+}-EVs maintained DHI

The sham group displayed a continuous DHI decrease, thus demonstrating successful IDD induction. BM-MSC-EV injection resulted in DHI reduction during the first eight weeks, with a slight non-significant increase at week 12. Interestingly, DHI in both NPC-EV groups did not display notable changes from baseline and was significantly higher than the sham and BM-MSC-EV groups ($p < 0.05$, Fig. 8).

NPC^{STD}-EVs and NPC^{Tie2+}-EVs preserved disc morphology

Gross IVD evaluation demonstrated significant degenerative alterations in the sham and BM-MSC-EV groups, while NPC^{STD}-EV and NPC^{Tie2+}-EV treatment preserved annulus fibrosus and nucleus pulposus morphology (Fig. 9a). Thompson scores for NPC^{STD}-EV- and NPC^{Tie2+}-EV-treated discs were significantly lower than in the sham and BM-MSC-EV

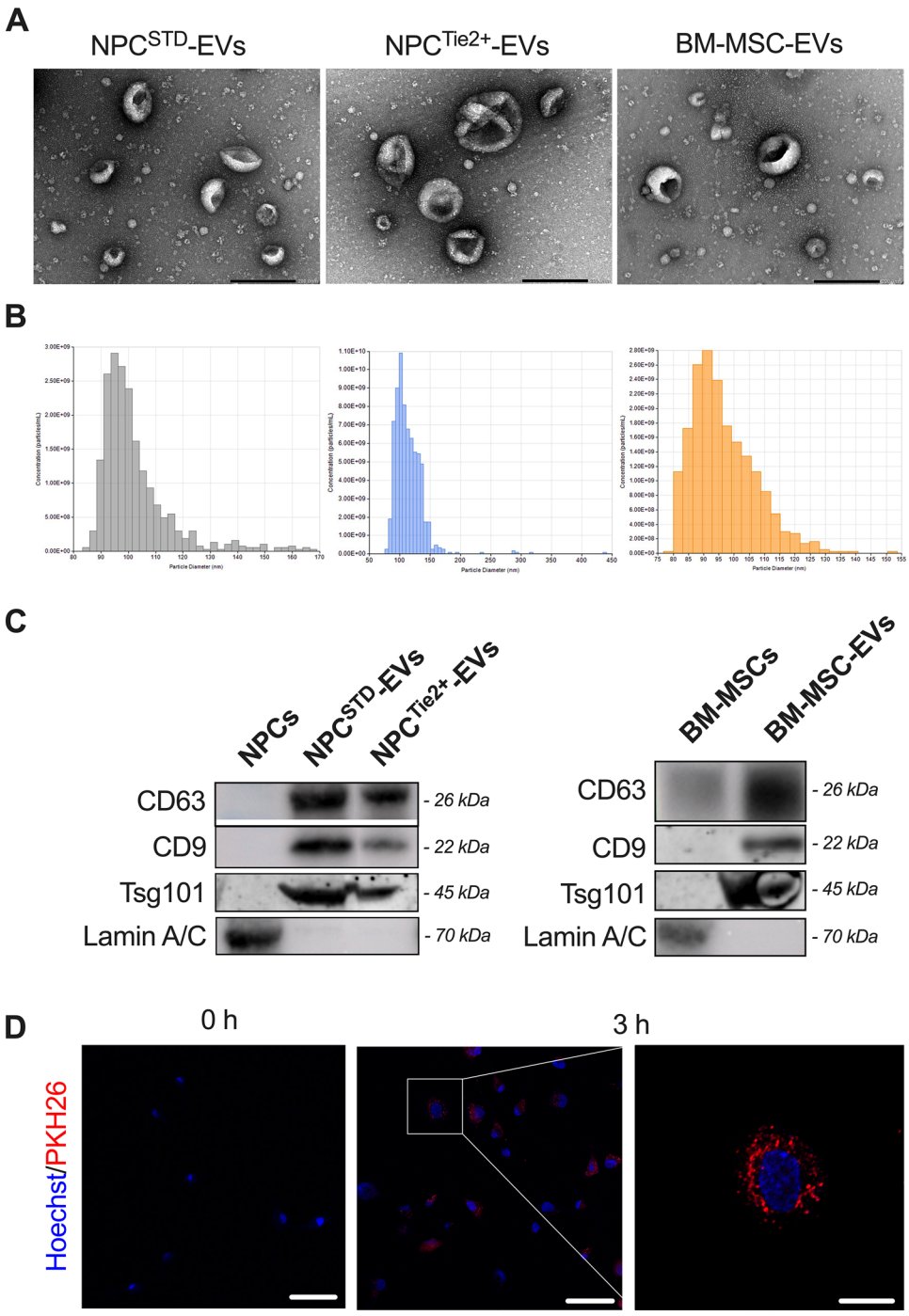

Fig. 3 Characterization of isolated EVs. **a** TEM images demonstrating the typical cup shape of purified EVs (scale bar = 200 nm). **b** EV size distribution showed that the highest abundance of nanoparticles was below 200 nm, thus designating them as exosomes. **c** Western blot of cell lysates and their EVs showing the expression of exosomal markers CD63, CD9, and TSG101 and the lack of the nuclear protein lamin A/C. **d** Observation of PKH26-labeled EVs (red) under confocal microscopy demonstrated the uptake of nanoparticles within dNPCs. dNPC nuclei were stained with Hoechst 33342 (blue). Scale bars = 50 µm (left and center); 20 µm (right). Representative images are shown. $N = 6$. Abbreviations: *dNPCs* degenerative nucleus pulposus cells, *EVs* extracellular vesicles, *TEM* transmission electron microscopy

groups ($p < 0.01$; Fig. 9b). Histological assessment confirmed these observations (Fig. 9c), with similarly lower scores for NPC^{STD}-EV and NPC^{Tie2+}-EV groups compared to both sham and BM-MSC-EV groups, although significant differences were obtained only compared to the former ($p < 0.05$; Fig. 9d).

Discussion

In this study, we showed that NPC-EVs were able to promote dNPC proliferation and reduce senescence in vitro while ameliorating pain and attenuating IDD in vivo. Moreover, we demonstrated that implementing a Tie2-enhancing protocol could augment NPC-EV therapeutic potential, emphasizing the importance of optimizing culture conditions.

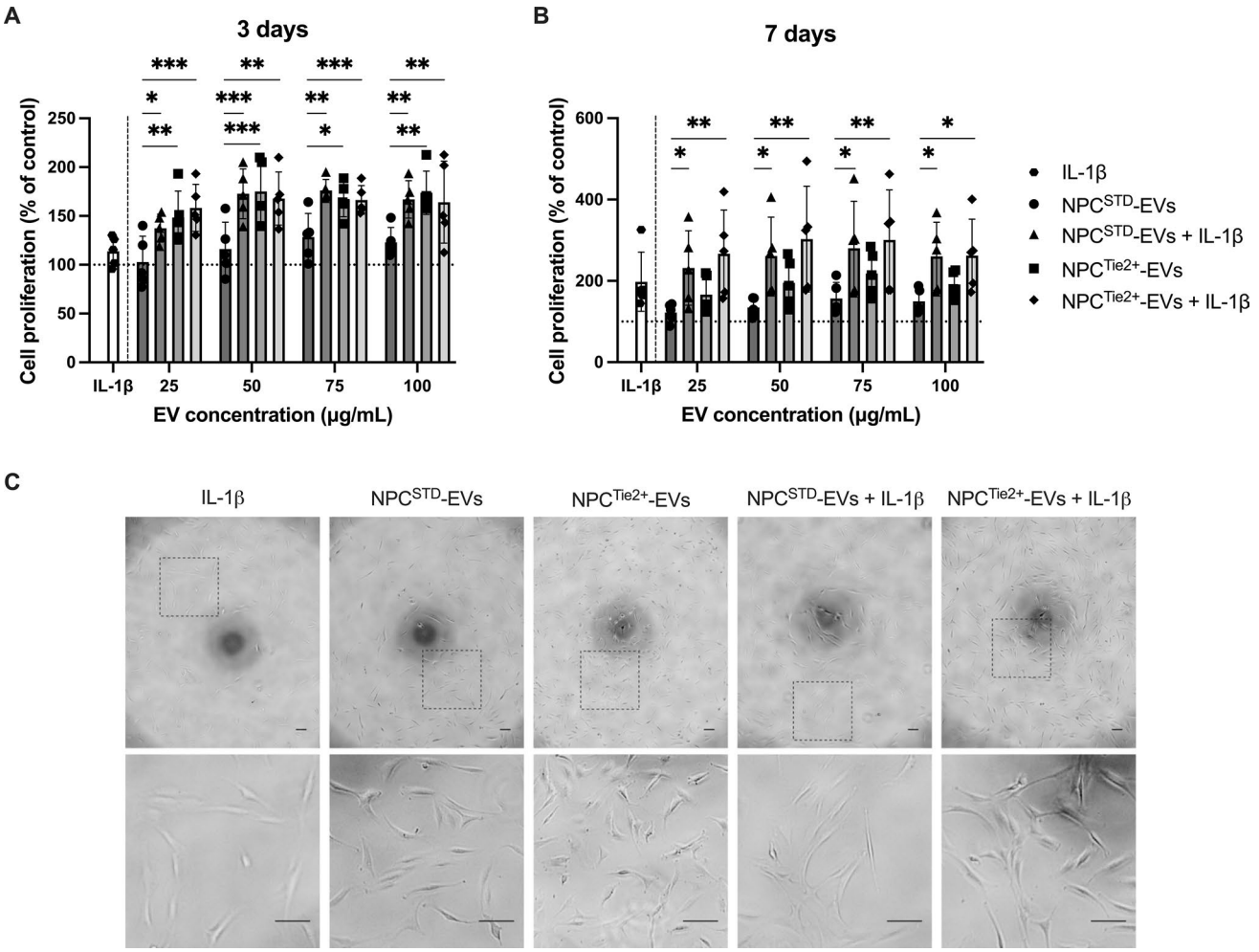

Fig. 4 Cell proliferation after treatment with NPC^{STD}-EVs and NPC^{Tie2+}-EVs with and without IL-1β detected by the CCK-8 assay at three (**a**) and seven days (**b**). Cell proliferation was calculated as percent absorbance change compared to the control group. Horizontal dotted lines correspond to a 100% viability compared to the control. $*p < 0.05$; $**p < 0.01$; $***p < 0.001$. $N = 5$. **c** Representative images of dNPCs at three days after culture. Despite a slight increase in proliferation, cells incubated with IL-1β showed an altered morphology as a possible consequence of a stress response. Conversely, dNPCs treated with NPC^{STD}-EVs and NPC^{Tie2+}-EVs displayed a normal cell shape, even in the presence of IL-1β. Scale bars = 100 µm. Abbreviations: *dNPCs*, degenerative nucleus pulposus cells; *IL-1β* interleukin-1β, *NPC^{STD}-EVs* extracellular vesicles isolated from nucleus pulposus cells cultured in standard conditions, *NPC^{Tie2+}-EVs* extracellular vesicles isolated from nucleus pulposus cells cultured in Tie2-enhancing conditions

Tie2 expression is associated with a progenitor phenotype characterized by multipotency and self-renewal capacity. The number of $Tie2^+$-NPCs decreases with age and advancing IDD, possibly explaining the progressive reduction of the IVD inherent self-repair capacity [7]. Therefore, $Tie2^+$-NPCs may constitute a potent cell source for IVD regeneration [11]. Recent evidence has demonstrated that EVs function as vectors of anabolic and anticatabolic mediators secreted by cells exploited as transplantation products to treat IDD. Indeed, EVs carry several biomolecules involved in cell communication, fate, and metabolism [18]. Furthermore, the EV cargo directly reflects the pathophysiological state of the donor cell, hence modulating the target cell response accordingly [27]. We postulated that increasing Tie2 expression in NPCs before EV isolation would promote the acquisition of a cargo with enhanced regenerative properties. According to our results, NPC^{Tie2+}-EVs exhibited the highest reparative capacity, although slightly superior to NPC^{STD}-EVs. By being isolated from relatively healthy NPCs, the intrinsic Tie2 expression and/or metabolic state of donor cells might equally result in the acquisition of an anabolic EV cargo.

Furthermore, our study revealed intriguing insights into pain-related behaviors. While the Von Frey test successfully demonstrated a reduction in mechanical hypersensitivity by NPC-EVs, other behavioral outcomes and systemic levels of IL-6 did not yield significant differences, similar to previous studies [22, 23]. This could be attributed to the specific

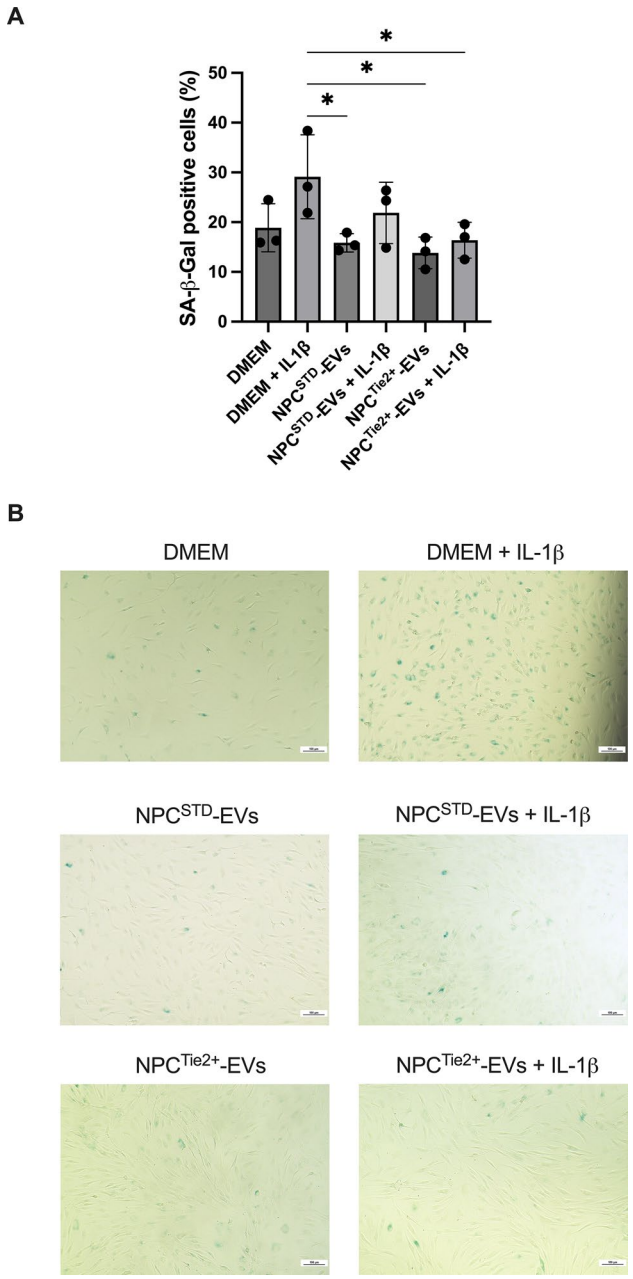

Fig. 5 dNPC senescence detected by SA-β-gal staining. NPC^{STD}-EVs and NPC^{Tie2+}-EVs significantly decreased the percentage of senescent cells compared to dNPCs cultured with IL-1β. Moreover, NPC^{Tie2+}-EVs prevented the increase in cell senescence despite the presence of IL-1β. $*p < 0.05$. $N = 3$. **b** Representative images of SA-β-gal-stained cells showing a reduced ratio of senescent cells in NPC-EV-treated samples. Blue cells: senescent cells. 10× magnification. Scale bars = 100 µm. Abbreviations: *dNPCs* degenerative nucleus pulposus cells, *IL-1β* interleukin-1β, *NPC^{STD}-EVs* extracellular vesicles isolated from nucleus pulposus cells cultured in standard conditions, *NPC^{Tie2+}-EVs* extracellular vesicles isolated from nucleus pulposus cells cultured in Tie2-enhancing conditions, *SA-β-gal* senescence-associated β-galactosidase

nature of tail IDD pain, which might not exert a substantial impact on overall behavior, especially considering the tail's limited weight-bearing role. Additionally, the acute degeneration model employed might not fully replicate the complex environment necessary to mimic discogenic pain [28].

Differently from previous studies, no significant beneficial outcomes of BM-MSC-EVs were found in vivo. Indeed, it has been earlier shown that BM-MSC-EVs were able to blunt ECM degradation, decrease disc cell loss, and dampen tissue inflammation and oxidative stress [18]. These differences could stem from several variables, including variations in cell sources, donor characteristics, and culture conditions. Nonetheless, while previous studies reported the use of repeated EV injections to achieve their therapeutic outcomes [18], a single injection of our NPC-derived EV product yielded a significant regenerative effect. These discrepancies, coupled with the wide variability among EV doses, units applied (protein vs. nanoparticle concentration), and inaccurate reporting in previous studies [18], emphasize the urgent need to establish an optimal dosing regimen for EV-based products.

While the caudal IVDs offer accessibility, established efficacy for evaluating intradiscally delivered treatments, and reproducibility, it is worth noting that the tail puncture model employed in this study has inherent limitations. Indeed, this model cannot fully replicate the complexity of chronic human lumbar IDD, particularly in terms of variations in cell types (such as notochordal cells in rats vs. human NPCs [29]) and biomechanical factors. These disparities may restrict the comprehensive understanding of the regenerative potential of our EV product in a real-world scenario. Another crucial factor to address is the xenogeneic nature of our EV transplantation (i.e., human to rat), potentially triggering an immunogenic response. However, our study did not find a reaction to our transplant product. This is in line with previous research that convincingly showed that EVs, either administered locally or systemically, did not provoke significant toxic or immunogenic reactions among different species [18, 30]. Therefore, we do not view this as a substantial concern. Although showing promising regenerative outcomes, the cargo of our EV product has not been specifically characterized. Unraveling the specific EV content will be essential to describe and predict its eventual effects. Moreover, additional in vitro experiments are needed to characterize the interaction between EVs and target cells, involved pathways, and mechanisms of action.

In summary, our study demonstrated NPC-EV therapeutic potential, highlighting the regenerative prowess of EVs isolated from NPC^{Tie2+}. These EVs countered

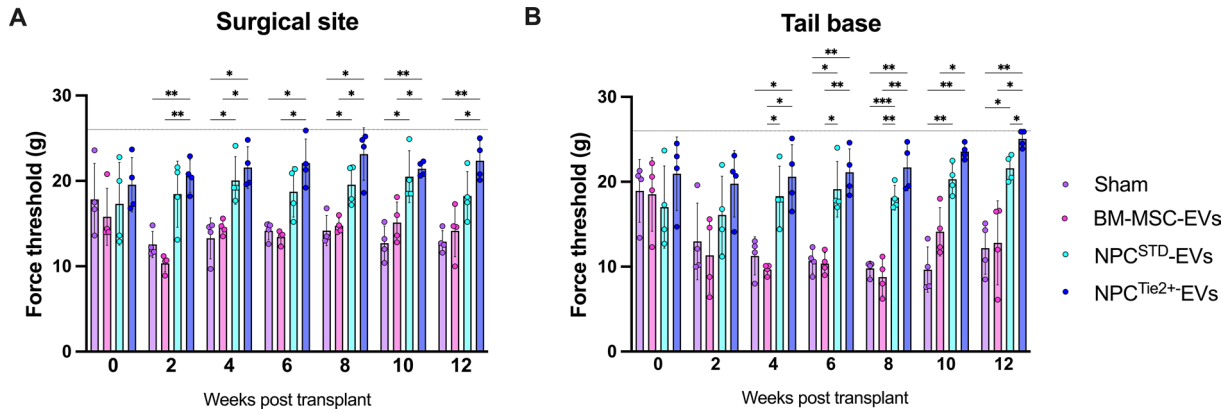

Fig. 6 Results of the Von Frey test to evaluate mechanical pain hypersensitivity at the surgical site (**a**) and tail base (**b**). Treatment with NPC^{STD}-EVs and NPC^{Tie2+}-EVs resulted in an increased pain threshold corresponding to a higher average force needed to elicit a withdrawal response compared to animals injected with BM-MSC-EVs or PBS. Horizontal dotted line: force threshold (26 g) able to induce a significant nocifensive response in rats. *$p<0.05$; **$p<0.01$; ***$p<0.001$. $N=4$ animals per group. Abbreviations: *BM-MSC-EVs* extracellular vesicles isolated from bone marrow-derived mesenchymal stromal cells, *NPC^{STD}-EVs* extracellular vesicles isolated from nucleus pulposus cells cultured in standard conditions, *NPC^{Tie2+}-EVs* extracellular vesicles isolated from nucleus pulposus cells cultured in Tie2-enhancing conditions, *PBS* phosphate-buffered saline

IL-1β-induced catabolic effects in vitro and preserved DHI and tissue morphology in vivo. Despite promising outcomes, clinical translation of EV products will demand extensive research, including cargo characterization and standardization.

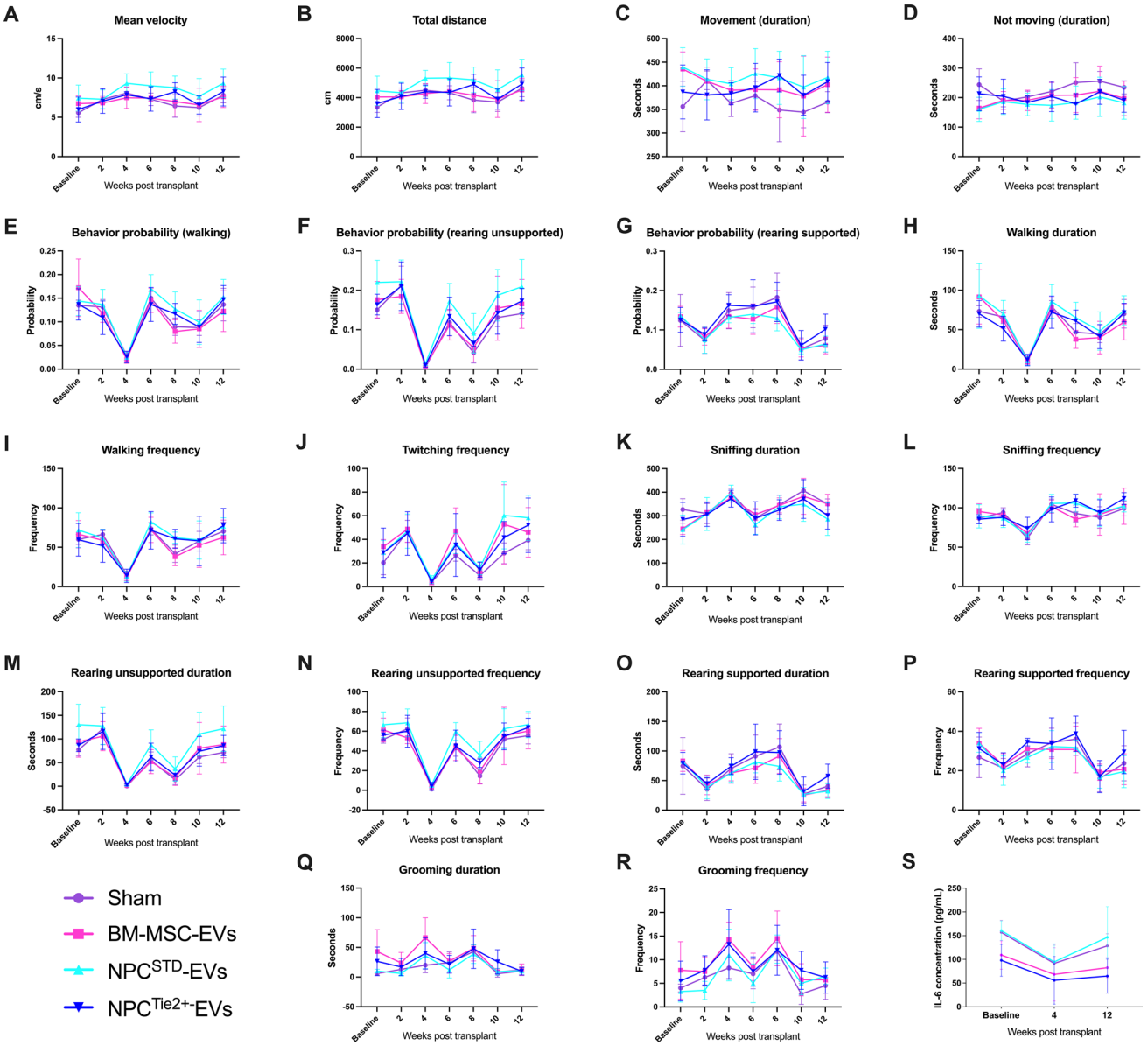

Fig. 7 Rat pain behaviors assessed by the open field test at baseline, 2-, 4-, 6-, 8-, 10-, and 12-weeks post-transplantation. Representative behavioral parameters evaluated included mean velocity (**a**), total distance (**b**), duration of movement (**c**), duration of not moving (**d**), probability of walking (**e**), probability of unsupported rearing (**f**), probability of supported rearing (**g**), walking duration (**h**), walking frequency (**i**), twitching frequency (**j**), sniffing duration (**k**), sniffing frequency (**l**), duration of unsupported rearing (**m**), frequency of unsupported rearing (**n**), duration of supported rearing (**o**), frequency of supported rearing (**p**), grooming duration (**q**), grooming frequency (**r**). (**s**) Serum concentration of IL-6 in treated animals at baseline and 1- and 3-months post-transplantation. $N = 4$ animals per group. Abbreviations: *IL* interleukin

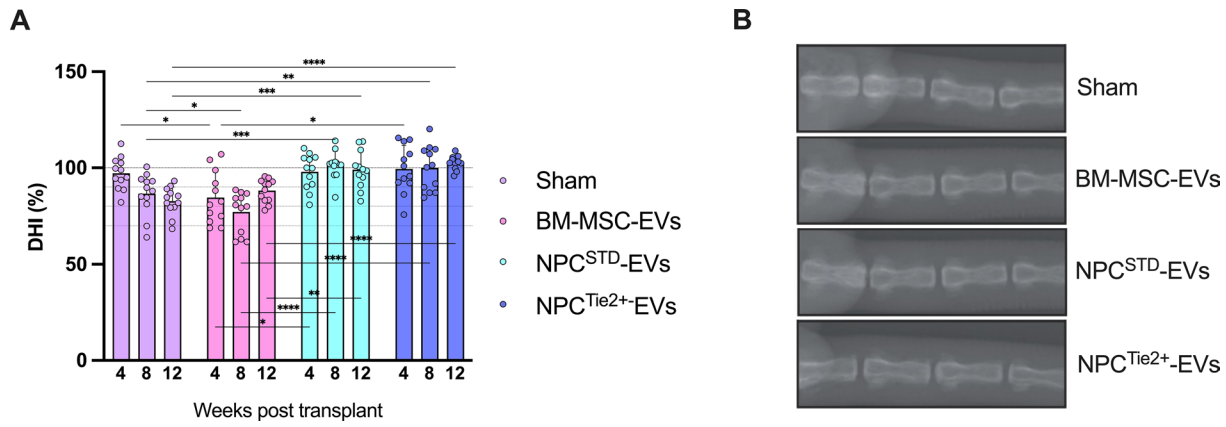

Fig. 8 Radiographic assessment of DHI changes at 4-, 8-, and 12-weeks post-transplantation compared to baseline. **a** DHI changes have been calculated as percent variation compared to baseline DHI. **b** Representative radiograms of rat tails at 12 weeks following treatment. *$p<0.05$; **$p<0.01$; ***$p<0.001$; ****$p<0.0001$. $N=12$ discs per group. Abbreviations: *DHI* disc height index

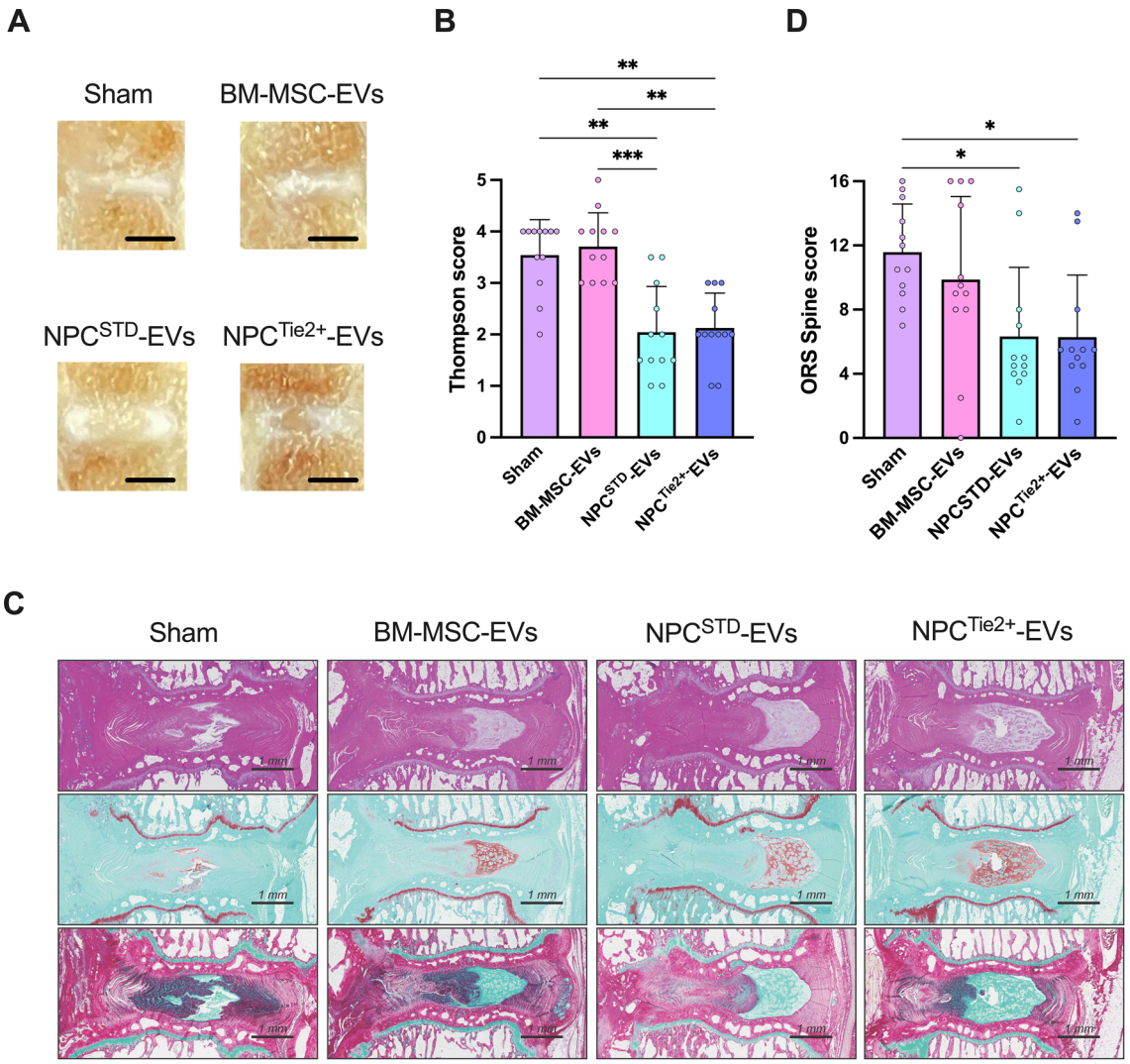

Fig. 9 Assessment of morphological changes following sham and EV injection. **a** Gross anatomical evaluation of dissected IVDs showed signs of advanced degenerative changes in the sham group and a notable reduction of disc height in the BM-MSC-EV group, with no clear difference between the AF and NP areas. Conversely, IVDs treated with NPC^{STD}-EVs and, especially, NPC^{Tie2+}-EVs displayed a preservation of the original IVD morphology with maintained disc height and demarcation of NP and AF. **b** The semiquantitative Thompson score of disc degenerative changes was significantly lower in IVDs injected with NPC^{STD}-EVs and NPC^{Tie2+}-EVs. Scale bars = 500 µm. **c** Histological sections of IVDs following hematoxylin–eosin (upper row), Safranin-O/Fast-Green (middle row), and Picrosirius-red/Alcian blue staining (lower row). NPC-EVs and, especially, NPC^{Tie2+}-EVs better preserved the NP morphology, proteoglycan content, and ECM structure compared to the other groups. Scale bars = 1 mm. **d** ORS Spine rat histological grading scores of sectioned IVDs. Representative images are shown. *$p < 0.05$; **$p < 0.01$; ***$p < 0.001$. $N = 12$ discs per group. Abbreviations: *AF* annulus fibrosus, *BM-MSC-EVs* extracellular vesicles isolated from bone marrow-derived mesenchymal stromal cells, *ECM* extracellular matrix, *EV* extracellular vesicle, *IVD* intervertebral disc, *NP* nucleus pulposus, *NPC^{STD}-EVs* extracellular vesicles isolated from nucleus pulposus cells cultured in standard conditions, *NPC^{Tie2+}-EVs* extracellular vesicles isolated from nucleus pulposus cells cultured in Tie2-enhancing conditions

Supplementary Information The online version contains supplementary material available at https://doi.org/10.1007/s00586-024-08163-3.

Acknowledgments The authors would like to thank Erika Matsushita, Takayuki Warita, Asami Kawachi, Takuma Araki, Misaki Higashiseto, Shunji Amano, Yuka Kitamura, Masatoshi Ito, Shuho Hori, Nahoko Fukunishi, and Ai Kotani for the support provided during the study. We would also like to acknowledge the Support Center for Medical Research and Education at Tokai University (Isehara, Japan) for their support with animal experimentation and sample processing.

Funding This study was supported by a grant from the ON Foundation, Switzerland, under the project n. 22–199 and by the "Patrizio Parisini" prize provided by the Italian Society of Spine Surgery & Italian Scoliosis Group (SICV&GIS).

Declarations

Conflict of interest HS is a paid employee of TUNZ Pharma Co., Ltd. (Osaka, Japan). DS is a scientific advisor of TUNZ Pharma Co., Ltd.

Ethical approval This study has been approved by the Institutional Review Board of Tokai University School of Medicine (Isehara, Kanagawa) under the approval number n. 221012. Informed consent for the collection and use of surgical waste products for research purposes was obtained from every patient. All animal experiments have been conducted according to ARRIVE guidelines and in respect of the 3R principle.

Open Access This article is licensed under a Creative Commons Attribution 4.0 International License, which permits use, sharing, adaptation, distribution and reproduction in any medium or format, as long as you give appropriate credit to the original author(s) and the source, provide a link to the Creative Commons licence, and indicate if changes were made. The images or other third party material in this article are included in the article's Creative Commons licence, unless indicated otherwise in a credit line to the material. If material is not included in the article's Creative Commons licence and your intended use is not permitted by statutory regulation or exceeds the permitted use, you will need to obtain permission directly from the copyright holder. To view a copy of this licence, visit http://creativecommons.org/licenses/by/4.0/.

References

1. Ferreira ML, de Luca K, Haile LM, Steinmetz JD, Culbreth GT, Cross M et al (2023) Global, regional, and national burden of low back pain, 1990–2020, its attributable risk factors, and projections to 2050: a systematic analysis of the Global Burden of Disease Study 2021. Lancet Rheumatol 5:e316–e329. https://doi.org/10.1016/s2665-9913(23)00098-x
2. Vadala G, Ambrosio L, Russo F, Papalia R, Denaro V (2021) Stem cells and intervertebral disc regeneration overview-what they can and can't do. Int J Spine Surg 15:40–53. https://doi.org/10.14444/8054
3. Tilotta V, Vadalà G, Ambrosio L, Cicione C, Di Giacomo G, Russo F et al (2023) Mesenchymal stem cell-derived secretome enhances nucleus pulposus cell metabolism and modulates extracellular matrix gene expression in vitro. Front Bioeng Biotechnol. https://doi.org/10.3389/fbioe.2023.1152207
4. Vadala G, Russo F, Ambrosio L, Di Martino A, Papalia R, Denaro V (2015) Biotechnologies and biomaterials in spine surgery. J Biol Regul Homeost Agents 29:137–147
5. Liang W, Han B, Hai Y, Sun D, Yin P (2022) Mechanism of action of mesenchymal stem cell-derived exosomes in the intervertebral disc degeneration treatment and bone repair and regeneration. Front Cell Dev Biol. https://doi.org/10.3389/fcell.2021.833840
6. Morita K, Schol J, Volleman TNE, Sakai D, Sato M, Watanabe M (2021) Screening for growth-factor combinations enabling synergistic differentiation of human msc to nucleus pulposus cell-like cells. Appl Sci. https://doi.org/10.3390/app11083673
7. Sakai D, Schol J, Bach FC, Tekari A, Sagawa N, Nakamura Y et al (2018) Successful fishing for nucleus pulposus progenitor cells of the intervertebral disc across species. Jor Spine. https://doi.org/10.1002/jsp2.1018
8. Guerrero J, Hackel S, Croft AS, Albers CE, Gantenbein B (2021) The effects of 3D culture on the expansion and maintenance of nucleus pulposus progenitor cell multipotency. JOR Spine 4:e1131. https://doi.org/10.1002/jsp2.1131
9. Li XC, Tang Y, Wu JH, Yang PS, Wang DL, Ruan DK (2017) Characteristics and potentials of stem cells derived from human degenerated nucleus pulposus: potential for regeneration of the intervertebral disc. BMC Musculoskelet Disord 18:242. https://doi.org/10.1186/s12891-017-1567-4
10. Sakai D, Nakamura Y, Nakai T, Mishima T, Kato S, Grad S et al (2012) Exhaustion of nucleus pulposus progenitor cells with ageing and degeneration of the intervertebral disc. Nat Commun 3:1264. https://doi.org/10.1038/ncomms2226
11. Sako K, Sakai D, Nakamura Y, Schol J, Matsushita E, Warita T et al (2021) Effect of whole tissue culture and basic fibroblast growth factor on maintenance of Tie2 molecule expression in human nucleus pulposus cells. Int J Mol Sci. https://doi.org/10.3390/ijms22094723
12. Soma H, Sakai D, Nakamura Y, Tamagawa S, Warita T, Schol J et al (2023) Recombinant laminin-511 fragment (iMatrix-511) Coating supports maintenance of human nucleus pulposus progenitor cells in vitro. Int J Mol Sci. https://doi.org/10.3390/ijms242316713
13. Basatvat S, Bach FC, Barcellona MN, Binch AL, Buckley CT, Bueno B et al (2023) Harmonization and standardization of nucleus pulposus cell extraction and culture methods. Jor Spine. https://doi.org/10.1002/jsp2.1238
14. Ito M, Kudo K, Higuchi H, Otsuka H, Tanaka M, Fukunishi N et al (2021) Proteomic and phospholipidomic characterization of extracellular vesicles inducing tumor microenvironment in Epstein-Barr virus-associated lymphomas. FASEB J. https://doi.org/10.1096/fj.202002730R
15. Thery C, Witwer KW, Aikawa E, Alcaraz MJ, Anderson JD, Andriantsitohaina R et al (2018) Minimal information for studies of extracellular vesicles 2018 (MISEV2018): a position statement of the International Society for Extracellular Vesicles and update of the MISEV2014 guidelines. J Extracell Vesicles 7:1535750. https://doi.org/10.1080/20013078.2018.1535750
16. Kakizaki M, Yamamoto Y, Otsuka M, Kitamura K, Ito M, Kawai HD et al (2020) Extracellular vesicles secreted by HBV-infected cells modulate HBV persistence in hydrodynamic HBV transfection mouse model. J Biol Chem 295:12449–12460. https://doi.org/10.1074/jbc.RA120.014317
17. Vadalà G, Di Giacomo G, Ambrosio L, Cicione C, Tilotta V, Russo F et al (2022) The effect of Irisin on human nucleus pulposus cells: new insights into the biological crosstalk between the muscle and intervertebral disc. Spine. https://doi.org/10.1097/brs.0000000000004488
18. DiStefano TJ, Vaso K, Danias G, Chionuma HN, Weiser JR, Iatridis JC (2021) Extracellular vesicles as an emerging treatment option for intervertebral disc degeneration: therapeutic potential, translational pathways, and regulatory considerations. Adv Healthc Mater. https://doi.org/10.1002/adhm.202100596
19. Mosley GE, Wang M, Nasser P, Lai A, Charen DA, Zhang B et al (2020) Males and females exhibit distinct relationships between intervertebral disc degeneration and pain in a rat model. Sci Rep 10:15120. https://doi.org/10.1038/s41598-020-72081-9
20. Schol J, Sakai D, Warita T, Nukaga T, Sako K, Wangler S et al (2022) Homing of vertebral-delivered mesenchymal stromal cells for degenerative intervertebral discs repair—an in vivo proof-of-concept study. Jor Spine. https://doi.org/10.1002/jsp2.1228

21. Barcellona MN, McDonnell EE, Samuel S, Buckley CT (2022) Rat tail models for the assessment of injectable nucleus pulposus regeneration strategies. Jor Spine. https://doi.org/10.1002/jsp2.1216
22. Lillyman DJ, Lee FS, Barnett EC, Miller TJ, Alvaro ML, Drvol HC et al (2022) Axial hypersensitivity is associated with aberrant nerve sprouting in a novel model of disc degeneration in female Sprague Dawley rats. Jor Spine. https://doi.org/10.1002/jsp2.1212
23. Wawrose RA, Couch BK, Dombrowski M, Chen SR, Oyekan A, Dong Q et al (2022) Percutaneous lumbar annular puncture: a rat model to study intervertebral disc degeneration and pain-related behavior. Jor Spine. https://doi.org/10.1002/jsp2.1202
24. Hiraishi S, Schol J, Sakai D, Nukaga T, Erickson I, Silverman L et al (2018) Discogenic cell transplantation directly from a cryopreserved state in an induced intervertebral disc degeneration canine model. Jor Spine. https://doi.org/10.1002/jsp2.1013
25. Thompson JP, Pearce RH, Schechter MT, Adams ME, Tsang IKY, Bishop PB (1990) Preliminary evaluation of a scheme for grading the gross morphology of the human intervertebral disc. Spine 15:411–415. https://doi.org/10.1097/00007632-199005000-00012
26. Lai A, Gansau J, Gullbrand SE, Crowley J, Cunha C, Dudli S et al (2021) Development of a standardized histopathology scoring system for intervertebral disc degeneration in rat models: an initiative of the ORS spine section. Jor Spine. https://doi.org/10.1002/jsp2.1150
27. Tilotta V, Vadalà G, Ambrosio L, Di Giacomo G, Cicione C, Russo F et al (2023) Wharton's Jelly mesenchymal stromal cell-derived extracellular vesicles promote nucleus pulposus cell anabolism in an in vitro 3D alginate-bead culture model. Jor Spine. https://doi.org/10.1002/jsp2.1274
28. Diwan AD, Melrose J (2022) Intervertebral disc degeneration and how it leads to low back pain. Jor Spine. https://doi.org/10.1002/jsp2.1231
29. Williams RJ, Laagland LT, Bach FC, Ward L, Chan W, Tam V et al (2023) Recommendations for intervertebral disc notochordal cell investigation: From isolation to characterization. Jor Spine. https://doi.org/10.1002/jsp2.1272
30. Zhu X, Badawi M, Pomeroy S, Sutaria DS, Xie Z, Baek A et al (2017) Comprehensive toxicity and immunogenicity studies reveal minimal effects in mice following sustained dosing of extracellular vesicles derived from HEK293T cells. J Extracell Vesicles. https://doi.org/10.1080/20013078.2017.1324730

Publisher's Note Springer Nature remains neutral with regard to jurisdictional claims in published maps and institutional affiliations.